THE JOURNAL OF PHYSICAL CHEMISTRY B

Article

pubs.acs.org/JPCB

Calculating Free Energy Changes in Continuum Solvation Models

Junming Ho*[,†,‡] and Mehmed Z. Ertem[§]

[†]Agency for Science, Technology and Research, Institute of High Performance Computing, 1 Fusionopolis Way, #16-16 Connexis, Singapore 138632

[‡]Department of Chemistry, Yale University, P.O. Box 208107, New Haven, Connecticut 06520, United States

[§]Chemistry Department, Brookhaven National Laboratory, Upton, New York 11973, United States

Supporting Information

ABSTRACT: We recently showed for a large data set of pK_as and reduction potentials that free energies calculated directly within the SMD continuum model compares very well with corresponding thermodynamic cycle calculations in both aqueous and organic solvents [*Phys. Chem. Chem. Phys.* **2015**, *17*, 2859]. In this paper, we significantly expand the scope of our study to examine the suitability of this approach for calculating *general* solution phase kinetics and thermodynamics, in conjunction with several commonly used solvation models (SMD-M062X, SMD-HF, CPCM-UAKS, and CPCM-UAHF) for a broad range of systems. This includes cluster-continuum schemes for pK_a calculations as well as various neutral, radical, and ionic reactions such as enolization, cycloaddition, hydrogen and chlorine atom transfer, and SN2 and E2 reactions. On the basis of this benchmarking study, we conclude that the accuracies of both approaches are generally very similar—the mean errors for Gibbs free energy changes of neutral and ionic reactions are approximately 5 and 25 kJ mol^{-1}, respectively. In systems where there are significant structural changes due to solvation, as is the case for certain ionic transition states and amino acids, the direct approach generally afford free energy changes that are in better agreement with experiment.

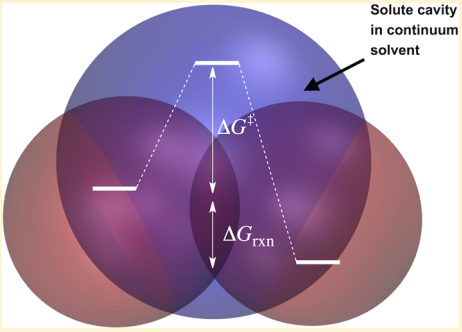

INTRODUCTION

Many important chemical reactions occur in the liquid phase, and the development of accurate methods to predict the energetics of solution phase reactions is an area of active research.[1] Toward this end, the introduction of continuum solvation models[2] (also known as implicit solvation models) marks an important milestone. These models have been parametrized to predict free energies of solvation of common neutral and ionic solutes that can be combined with experimental or *ab initio* gas phase energies to estimate free energy changes in solution. Such procedures have been widely applied in the computation of kinetic and thermodynamic properties such as rate coefficients,[3] pK_as,[4] reduction potentials,[5] and binding energies[6] in various solvents.

The *intrinsic* free energy of solvation corresponds to the change in Gibbs free energy of the solute in the gas and solution phase. For charged solutes, this differs from the *real* free energy of solvation that also includes contribution from the surface potential of the solvent. As discussed elsewhere,[7] continuum solvation models predict intrinsic free energies of solvation (ΔG_S) using the expression shown in eq 1a. In eq 1b, E_{soln} and E_{gas} are the solute electronic energy in the solution and gas phase computed on geometries optimized in the respective phases so that it includes the effect of geometrical relaxation in the free energy of solvation. G^{corr} denotes the thermal contribution to the Gibbs free energy, and G_{nes} is the nonelectrostatic component of the free energy of solvation. The latter includes the dispersion−repulsion−cavitation and solvent structural terms associated with solvation. The gas phase and solution phase optimized geometries are labeled as $\mathbf{R}_g$ and $\mathbf{R}_l$, respectively.

$$\Delta G_S = G_{soln}(\mathbf{R}_l) - G_{gas}(\mathbf{R}_g) \tag{1a}$$

$$\Delta G_S = E_{soln}(\mathbf{R}_l) - E_{gas}(\mathbf{R}_g) + G^{corr}_{soln}(\mathbf{R}_l) - G^{corr}_{gas}(\mathbf{R}_g) + G_{nes}(\mathbf{R}_l) \tag{1b}$$

$$E_{soln} = \left\langle \Psi^{pol} \middle| H^{\circ} + \frac{V}{2} \middle| \Psi^{pol} \right\rangle \tag{1c}$$

It is generally assumed for the purpose of parametrization that thermal contributions to the solute Gibbs free energy are sufficiently similar in the gas and solution phase for small rigid solutes.[2a,b] This eliminates the need for costly Hessian calculations, and solvation free energies are usually calculated using eq 2.[8] Consequently, any noncanceling differences in the gas and solution phase thermal corrections (e.g., conversion of gas phase rotation to liquid phase librations) are implicitly incorporated into the solvation model through parametrization.[8,9] In systems where solvation-induced changes in thermal

Received: January 6, 2016
Revised: January 26, 2016
Published: January 27, 2016

DOI: 10.1021/acs.jpcb.6b00164
J. Phys. Chem. B 2016, 120, 1319−1329

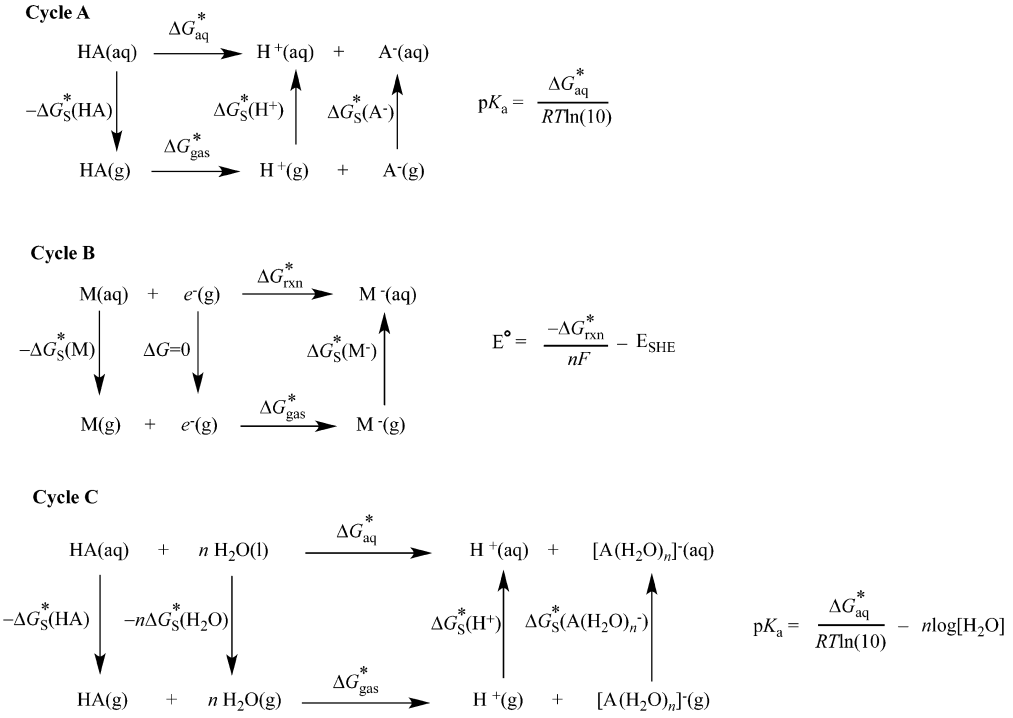

Figure 1. Common thermodynamic cycles used for calculating pK_as and reduction potentials.

motions (e.g., vibrational frequencies) are significant, eq 1 is presumably more accurate because these changes are explicitly accounted for in the calculated free energy of solvation.

$$\Delta G_S = E_{soln}(\mathbf{R_l}) - E_{gas}(\mathbf{R_g}) + G_{nes}(\mathbf{R_l}) \quad (2)$$

In thermodynamic cycle calculations, the solution phase free energy is obtained as the sum of the gas phase Gibbs free energy and free energy of solvation (eq 3a). The former is usually calculated at a rigorous level of theory, and the free energy of solvation is evaluated at the level of theory that is consistent with the parametrization of the solvation model. In general, continuum solvation models are parametrized at Hartree−Fock (HF) or density functional theory (DFT) levels in conjunction with a small basis set that are commonly used to evaluate geometries and frequencies but are not suitable for accurate calculation of gas phase energies. In eq 3a, the superscript "H" denotes that the energy is based on a single point calculation at a high level of theory (e.g., benchmarked composite procedures such as G3(MP2)[10] or CBS-QB3[11]), and "L" is a lower-level method (e.g., HF or DFT with a double-ζ basis set) used to evaluate the geometry and thermal corrections. Substituting eq 1b for the free energy of solvation in eq 3a yields the solution phase free energy in eq 3b.

$$G_{soln}(\mathbf{R_l}) = G^{H}_{gas}(\mathbf{R}_g) + \Delta G^{L}_{S} \quad (3a)$$

$$G_{soln}(\mathbf{R_l}) = E^{H}_{gas}(\mathbf{R_g}) + E^{L}_{soln}(\mathbf{R_l}) + G^{corr,L}_{soln}(\mathbf{R_l}) - E^{L}_{gas}(\mathbf{R_g}) + G^{L}_{nes}(\mathbf{R_l}) \quad (3b)$$

In a recent study,[12] we examined an alternative protocol where solution phase free energies are obtained directly from electronic structure calculations carried out in the continuum solvent reaction field only. Additionally, the thermal contributions to the solution phase Gibbs free energy G^{corr}_{soln} were obtained using partition functions derived from the ideal gas rigid-rotor harmonic oscillator approximation. For a single-conformation molecule, the thermal contribution evaluated in a continuum solvation model may be partitioned into electronic, liberational, librational, and vibrational free energies shown in eq 4a.[9] The resulting expression for the solution phase free energy is shown in eq 4b, and we will refer to it as the *direct approach* in this paper.

$$G^{corr,L}_{soln}(\mathbf{R_l}) = G^{L}_{soln}(elec) + G^{L}_{soln}(liber) + G^{L}_{soln}(libra) + G^{L}_{soln}(vib) \quad (4a)$$

$$G_{soln}(\mathbf{R_l}) = E^{H}_{soln}(\mathbf{R_l}) + G^{L}_{nes}(\mathbf{R_l}) + G^{corr,L}_{soln}(\mathbf{R_l}) \quad (4b)$$

We have employed both free energy expressions to evaluate the acidity constants (pK_as) and standard reduction potentials ($E°$) using the SMD-M062X continuum solvation model. For a large test set of aqueous 83 pK_as and 42 reduction potentials, the mean difference between the thermodynamic cycle and direct approaches is approximately 2.5 kJ mol^{-1}.[12] This difference is significantly smaller than the mean accuracy associated with continuum solvent protocols for calculating pK_as and reduction potentials. In systems where solvation induced changes in structure are significant, we found that the direct approach provided a substantial improvement presumably because the high-level single-point calculations are carried out in the solution phase on corresponding optimized geometries. The study suggested that the direct approach may provide a more general and reliable alternative to thermodynamic cycles for the calculation of solution phase pK_as and reduction potentials.

In the present work, we wish to further investigate the scope of the direct approach for the calculation of *general* solution phase kinetics and thermodynamics and its performance with respect to other continuum solvation models and choice of electronic structure methods. Frau and co-workers have investigated the quality of both direct and thermodynamic cycle approaches for calculating the aqueous pK_as of a small test

DOI: 10.1021/acs.jpcb.6b00164
J. Phys. Chem. B 2016, 120, 1319−1329

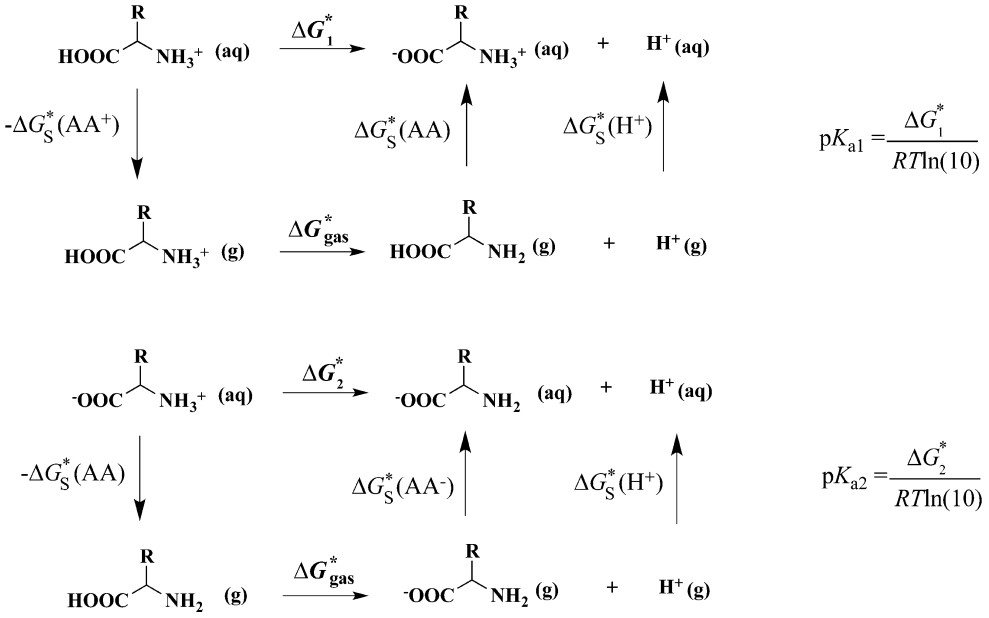

Figure 2. Thermodynamic cycles used to compute the first and second pK_as of amino acids.

set of organic compounds using a proton exchange scheme.[13] However, these studies were generally focused on a specific class of reactions and combination of solvation model and electronic structure theory method. A broader study that examines the performance of both approaches toward predicting the energies and barriers of various types of reactions is still needed. To this end, we have included several other commonly used solvation models (SMD-HF and CPCM-UAKS/UAHF), and the data set is also significantly expanded to cover a broad range of systems and reaction types. This includes, in addition to the original data set of pK_as and reduction potentials, various pericyclic, tautomerization, radical (hydrogen and halogen abstraction), and ionic (SN2, E2, and Michael addition) reactions. This diverse data set will provide a rigorous assessment of the suitability of the direct approach for the calculation of general solution phase kinetics and thermodynamics.

This paper is organized as follows: we first review the theory for both direct and thermodynamic cycle calculation of solution phase energetics, issues relating to standard states, and details of our test set and computational methods. This is followed by results and discussion, where the performance of both approaches for the prediction of solution phase thermochemistry for the various types of reactions is examined. The origin of the agreement (and disagreement) between the two approaches is explained, and we conclude with a discussion of some possible directions for future work.

THEORY

In our previous study,[12] we presented the derivation for the expressions used to calculate pK_as and reduction potentials based on cycles A and B in Figure 1. To briefly recap, we showed (using cycle A in Figure 1 as example) that when the free energies of solvation are evaluated using eq 1b, the resulting expression for the deprotonation free energy is given by eq 5. The corresponding expression for the direct approach is shown in eq 6. The superscripts "∗" and "o" denote that the quantities are computed at a standard state of 1 mol L^{-1} and 1 atm, and the last term in eqs 5 and 6 is the Gibbs free energy change for converting between standard states $\Delta G^{o\rightarrow *}$. Other symbols in these expressions have their usual meanings.

$$\Delta G^{*}_{soln}(TC) = \Delta E^{[L]}_{soln} + \Delta G^{o[L]}_{corr,soln} + \Delta E^{[H]}_{gas} - \Delta E^{[L]}_{gas} + G^{o}_{soln}(H^+) + \Delta G^{o\rightarrow *} \quad (5)$$

$$\Delta G^{*}_{soln}(direct) = \Delta E^{[H]}_{soln} + \Delta G^{o[L]}_{corr,soln} + G^{o}_{soln}(H^+) + \Delta G^{o\rightarrow *} \quad (6)$$

$$\Delta E^{[X]} = E^{[X]}(A^-) - E^{[X]}(HA) \quad (7a)$$

$$\Delta G^{o[X]}_{corr,soln} = G^{o[X]}_{corr,soln}(A^-) - G^{o[X]}_{corr,soln}(HA) \quad (7b)$$

$$\Delta G^{o\rightarrow *} = RT\ \ln\left(\frac{RT}{P}\right) \quad (7c)$$

All geometries and thermal corrections are evaluated at a lower level of theory (L), and the electronic energies are obtained through a high-level (H) single point calculation (E_{soln} includes G_{nes}). In the direct approach, the high-level calculations are carried out directly on the solution phase optimized geometry in the presence of the solvent reaction field, whereas these are carried out on gas phase optimized geometries in the thermodynamic cycle approach. In this work, the lower level of theory (L) is determined by the electronic structure method used to parametrize the continuum solvation model. The SMD model is optimized at several levels of theory including HF and M06-2X. For the CPCM-UAKS and CPCM-UAHF models, we have employed the B3LYP and HF levels of theory, respectively. For consistency with our earlier study, the G3(MP2)-RAD(+) procedure[14] is used as the high level of theory. This procedure is abbreviated as "G(+)" from here on.

Cycle A has also been used to compute the first and second pK_as of a group of amino acids. For this class of compounds, the reader should note that the zwitterions are not stationary points on the gas phase potential energy surface (with the exception of optimized structures at HF level),[15] and their free energies of solvation are computed as the transfer of a neutral amino acid in the gas phase to its zwitterion in the aqueous phase (Figure 2). Additionally, we have examined alternative

DOI: 10.1021/acs.jpcb.6b00164
J. Phys. Chem. B 2016, 120, 1319−1329

schemes for calculating pK_as. Notably, we have employed cycle C in Figure 1 that involves explicit solvation of ions with 1−3 water molecules. In this cluster-continuum approach,[4i] the expressions for the deprotonation free energy are shown in eqs 8 and 9 where n is the number of water molecules and $[H_2O]$ is the concentration of bulk water. The last term in these equations is needed because the standard state of bulk water is 55.5 mol L^{-1}. The reader is referred to several earlier papers[4a,16] for a more thorough discussion of standard states involving explicit water molecules.

$$\Delta G^{*}_{soln}(TC) = \Delta E^{[L]}_{soln} + \Delta G^{o[L]}_{corr,soln} + \Delta E^{[H]}_{gas} - \Delta E^{[L]}_{gas} + G^{o}_{soln}(H^+) + (1-n)\Delta G^{o\rightarrow *} - nRT\ln([H_2O]) \quad (8)$$

$$\Delta G^{*}_{soln}(direct) = \Delta E^{[H]}_{soln} + \Delta G^{o[L]}_{corr,soln} + G^{o}_{soln}(H^+) + (1-n)\Delta G^{o\rightarrow *} - nRT\ln([H_2O]) \quad (9)$$

Data Set. Table 1 provides an overview of the data set of molecules used in this benchmarking study. Where possible, we have included systems with experimental data. This data set covers a range of neutral, radical, and ionic reactions. Details of the test set of reaction barriers are shown in Scheme 1.

Table 1. Overview of Data Set

thermodynamics	N^a	ref
pK_a (organic)	69 (22)[b]	4a, 4b, 17
pK_a (inorganic)	14	4a
pK_a (amino acids)	8	12
reduction potentials	42	5a
keto−enol tautomerization	30	18
atom-abstraction reactions	12	19
kinetics	N^a	ref
ionic reactions	44	20
pericyclic reactions	18	21
radical reactions	21	3a, 19, 22

[a]Number of molecules in data set. [b]A subset of 22 organic acids were examined using the cluster-continuum scheme shown in Figure 1 (cycle C).

COMPUTATIONAL DETAILS

All electronic structure calculations in this work were carried out using the Gaussian 09[23] software package. The test set of molecules and their starting geometries were obtained from the references cited in Table 1. For the SMD-M062X,[24] CPCM-UAKS,[25] SMD-HF,[24] and CPCM-UAHF[26] models, all geometries, thermal corrections, and free energies of solvation were evaluated at the M06-2X,[27] B3LYP,[28] and HF in conjunction with the 6-31+G(d) basis set,[29] respectively. Vibrational analyses confirmed that all reactants and products have zero imaginary frequencies and that transition states are true first-order saddle points on the potential energy surface. Free energies of solvation were evaluated using eq 1 where gas phase and solution phase calculations were carried out on geometries optimized in their respective phases. For open-shell species, the SMD-HF and CPCM-UAHF free energies of solvation were obtained from (RO)HF/6-31+G(d) single-point calculations on UHF optimized geometries as the latter sometimes yielded unphysical free energies of solvation due to spin contamination. High-level single-point calculations were carried out using the G3(MP2)-RAD(+) procedure,[14] where "(+)" denotes that calculations involving the 6-31G(d) basis set in the original G3(MP2)-RAD procedure were replaced with 6-31+G(d) so as to provide an improved description of anionic species. In this procedure, CCSD(T) and MP2 calculations carried out within the continuum solvation model were based on the noniterative energy only scheme where the solvated HF orbitals are used to calculate the correlation energy.[30]

All thermal corrections to the Gibbs free energy of solvation were computed using the ideal gas molecular partition functions in conjunction with the rigid-rotor quasiharmonic oscillator (RR-QHO) approximation. In the QHO approximation,[9] vibrational frequencies that were lower than 100 cm^{-1} were raised to 100 cm^{-1} due to the breakdown of the harmonic oscillator for low-frequency modes. In all calculations involving the CPCM model, we enabled the following keywords (Dis, Cav, Rep, Alpha 1.2) in Gaussian09 in order to obtain free energies of solvation that are in accord with their original parametrization. All SMD calculations were carried out using the default settings in Gaussian09.

In the pK_a calculations, it is important to use the proton free energy of hydration that is consistent with the parametrization of the solvation model.[6a,7] Accordingly, we have employed $\Delta G^{*}_{S}(H^+)$ of −1112.5 kJ mol^{-1} for the SMD and CPCM-UAKS models and −1093.7 kJ mol^{-1} for the CPCM-UAHF model. Similarly, the E_{SHE} value of 4.28 V is employed for the SMD and CPCM-UAKS models and 4.47 V for CPCM-UAHF. See refs 5a and 7 for a more thorough discussion of the choice of proton solvation free energy in continuum solvent calculation of pK_as and reduction potentials. The value of −0.86 kcal mol^{-1} for the gas phase energy of the electron based on the Fermi−Dirac statistical formalism is employed.[5a]

RESULTS AND DISCUSSION

Aqueous pK_as and Standard Reduction Potentials. The aqueous pK_as and standard reduction potentials of various classes of compounds (alcohols, amines, carboxylic acids, inorganic acids, carbon acids, and cationic acids) were calculated using both direct and thermodynamic cycle (TC) approaches. Full details of the test set are provided in the Supporting Information. Figure 3 compares the pK_as calculated using the two approaches. As shown, there is generally very good agreement between the pK_as from both approaches, where the overall mean absolute deviations (MAD) are 0.4, 1.0, 0.5, and 1.1 pH units for the SMD-M062X, SMD-HF, CPCM-UAKS and CPCM-UAHF models, respectively. The corresponding maximum absolute deviations (AD_{max}) are 0.9, 3.3, 2.1, and 4.3 pH units. The reduction potentials show a similar trend where the MADs are 28, 63, 41, and 63 mV, respectively. The corresponding AD_{max} are 74, 210, 205, and 250 mV. It appears that HF-based solvation models (i.e., SMD-HF and CPCM-UAHF) give rise to larger deviations, especially for alcohols and carboxylic acids.

Tables 2 and 3 summarize the mean absolute *error* (MAE) of calculated pK_as and reduction potentials *with respect to experimental data* for each class of compound. For DFT-based solvation models (SMD-M062X and CPCM-UAKS), it is evident that the accuracies of directly calculated pK_as and reduction potentials are very comparable to those obtained using the corresponding thermodynamic cycle. Notably, the MAEs from both approaches differ by less than 0.8 pH units (pK_as) or 50 mV (reduction potentials) for all classes of

DOI: 10.1021/acs.jpcb.6b00164
J. Phys. Chem. B 2016, 120, 1319−1329

Scheme 1

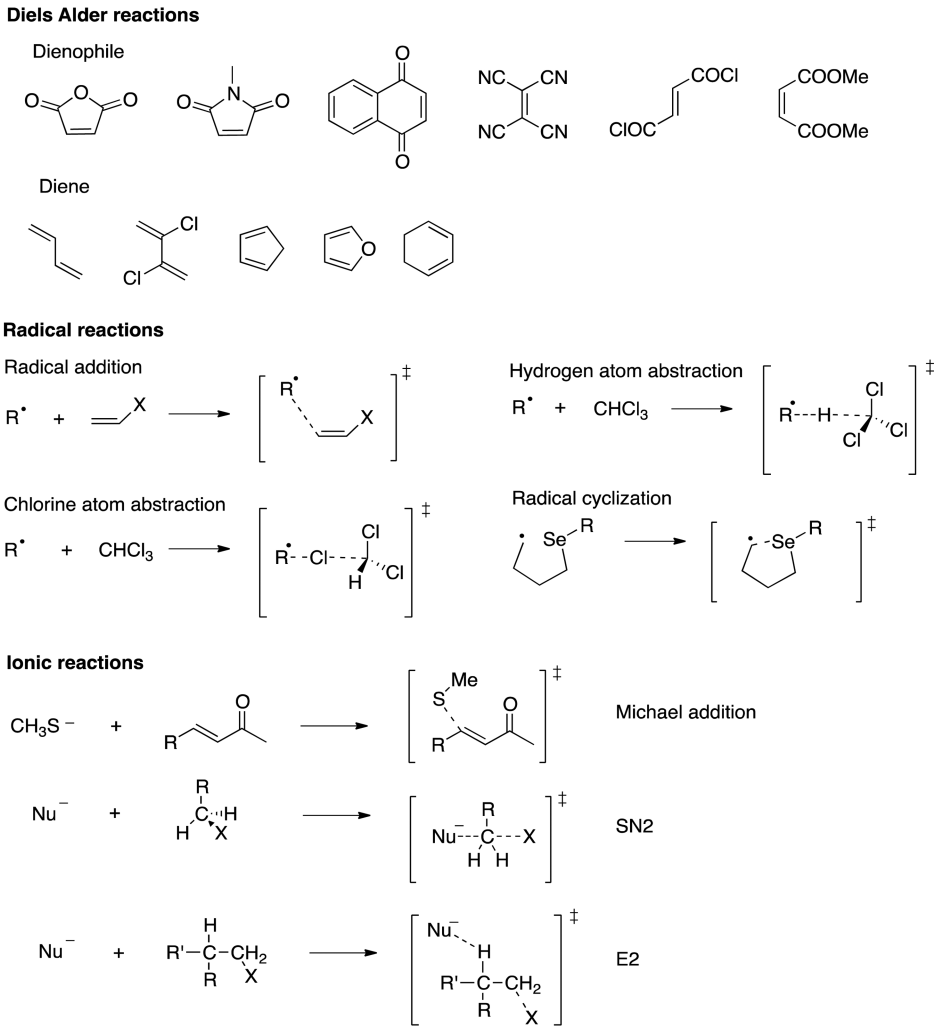

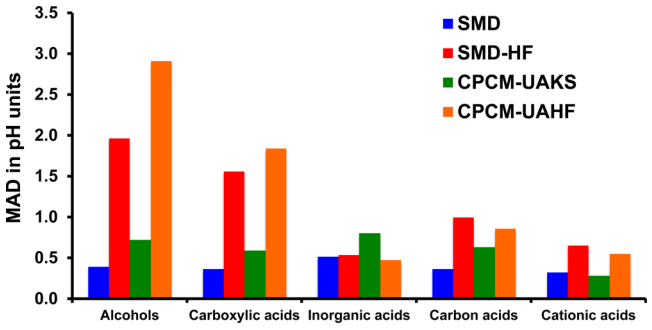

Figure 3. Mean absolute deviations between pK_as calculated using TC and direct approach.

compounds. This difference is significantly smaller than the mean accuracy of the calculations (ca. 4−7 pH units for pK_as and 250−320 mV for reduction potentials) as shown in Tables 2 and 3. In the case of HF-based solvation models (SMD-HF and CPCM-UAHF), the TC approach led to mean errors that are significantly lower for oxygen-centered acids (alcohols and carboxylic acids). For example, the MAEs of the TC approach are approximately 2−3 units lower than the direct approach for alcohols (Table 2). On the other hand, the reduction potentials for alcohols display very similar MAEs for the two approaches.

It is of interest to examine why the HF-based models display larger deviations and why the TC approach gave better agreement with experiment for these systems. To shed light on this question, one can quantify the deviation between the deprotonation (or reduction) free energies from the two approaches as the difference of eqs 5 and 6. It is straightforward to show that this difference can be expressed in terms of the solvation contribution $\Delta\Delta G_S^*$ to the deprotonation free energy, where L and H denote the levels of theory used to evaluate the free energies of solvation:

$$\Delta\Delta G^*_{soln} = \Delta G^*_{soln}(\mathrm{TC}) - \Delta G^*_{soln}(\mathrm{direct}) \quad (10a)$$

$$\Delta\Delta G^*_{soln} = \Delta\Delta G_S^{*[\mathrm{L}]} - \Delta\Delta G_S^{*[\mathrm{H}]} \quad (10b)$$

$$\Delta\Delta G_S^{*[\mathrm{X}]} = [\Delta G_S^{*[\mathrm{X}]}(\mathrm{A}^-) - \Delta G_S^{*[\mathrm{X}]}(\mathrm{HA})] \quad (10c)$$

Accordingly, if $\Delta\Delta G_S^*$ was invariant to the choice of electronic structure theory method, then the deprotonation free energies from direct and TC approaches would be identical. Thus, the deviation in eq 10a reflects changes in $\Delta\Delta G_S^*$ as the electronic description is improved from "L" to "H". It should be stressed that eq 10a does not provide any direct information concerning the relative accuracy of the two approaches.

Table 4 compares the free energies of solvation for selected systems calculated using the SMD-HF and SMD-M062X

DOI: 10.1021/acs.jpcb.6b00164
J. Phys. Chem. B 2016, 120, 1319−1329

Table 2. Mean Absolute Error (in pH Units) between Calculated pK_as and Experiment

		SMD-M062X[b]		SMD-HF		UAKS		UAHF	
system	N[a]	direct	TC	direct	TC	direct	TC	direct	TC
alcohols	13	8.0	7.8	7.5	5.5	7.3	8.0	10.8	7.0
carboxylic acids	7	2.3	2.0	2.2	1.2	3.3	3.9	6.1	4.2
inorganic acids	14	5.3	5.1	4.2	4.3	3.5	4.2	7.5	7.3
carbon acids	21	6.5	6.3	6.0	5.2	6.7	7.1	10.5	9.8
cationic acids	28	2.3	2.2	2.6	2.3	2.8	2.8	3.1	2.9
overall MAE		4.7	4.6	4.5	3.8	4.6	5.1	7.1	6.2
AE_{max}		8.8	9.0	8.8	8.3	10.3	11.1	14.8	14.1

[a]Number of molecules in data set. [b]Data from ref 12.

Table 3. Mean Absolute Error (in eV) between Calculated $E°$ and Experiment

		SMD-M062X[b]		SMD-HF		UAKS		UAHF	
system	N[a]	direct	TC	direct	TC	direct	TC	direct	TC
amines	14	0.09	0.10	0.07	0.10	0.15	0.17	0.13	0.15
alcohols	24	0.36	0.36	0.38	0.36	0.26	0.31	0.45	0.37
nitroxides	4	0.15	0.10	0.09	0.07	0.03	0.04	0.14	0.14
overall MAE		0.25	0.25	0.26	0.25	0.20	0.24	0.32	0.28
AE_{max}		0.68	0.67	0.67	0.62	0.60	0.65	0.73	0.56

[a]Number of molecules in data set. [b]Data from ref 12.

models. In each model, the G3(MP2)-RAD(+) (abbreviated as G(+) from here on) free energies of solvation are determined from single-point calculations on geometries optimized at the HF and M06-2X/6-31+G(d) levels, respectively. Closer inspection explains why the direct method deviates significantly from the TC approach for the SMD-HF model for these systems. Notably, the HF free energies of solvation are consistently more exergonic than G(+) values, *particularly for anions*. By comparison, the deviations between M06-2X and G(+) values are very similar for both neutrals and anions. Using the methanol/methoxide system as an example, the HF free energies of solvation are 7 and 21 kJ mol^{-1} more negative than the G(+) values, respectively. For the M06-2X calculations, the corresponding deviations are 6 and 9 kJ mol^{-1}. Consequently, the deprotonation free energies from TC and direct approaches deviate by about 14 and 3 kJ mol^{-1} for the SMD-HF and SMD-M062X models, respectively. As such, the larger deviations observed in HF-based solvation models are due to the asymmetry in the deviation between HF and G(+) free energies of solvation for the reactant (neutral) and product (anion), where the HF values are significantly more negative for the latter. This is presumably because HF tends to result in a solute wave function that is over polarized.[31] Consequently, larger changes in $\Delta\Delta G_S^*$ can be expected when HF is replaced by a higher level of theory (Table 4). Interestingly, direct and TC approaches yield very similar reduction potentials for all classes of compounds, including oxygen-centered radicals (Table 3). This is because the (RO)HF free energies of solvation for the radical and reduced anion show a similar deviation to their G(+) values, and therefore the resulting $\Delta\Delta G_S^*$ calculated at both levels of theory are very similar. For example, the (RO)HF free energies of solvation for the para-*N*,*N*-dimethylaniline radical and anion are both approximately 20 kJ mol^{-1} more negative compared to the G(+) values (Table 4).

Comparison of SMD-M062X and SMD-HF pK_as evaluated by the TC approach (Table 2) shows that this overpolarization effect of HF actually improves accuracy (except for cationic acids). This is because continuum solvation models generally underestimate (less negative) the free energies of solvation of anions, and this deficiency is partially compensated by the HF method. As shown in Table 4, HF generally delivers ionic free energies of solvation and $\Delta\Delta G_S^*$ that are in better agreement with experiment compared to M06-2X or G(+). In the original SMD paper,[24] the mean absolute error for HF is approximately 4−10 kJ mol^{-1} smaller than those obtained at M06-2X and B3LYP for a test set of 60 aqueous anionic free energies of solvation. For cations, the mean absolute error for HF and M06-2X are within 3.5 kJ mol^{-1}. The latter also explains why the pK_as of cationic acids are very similar for SMD-M062X and SMD-HF models.

In this context, it is interesting that the TC-UAHF approach did not perform better than its UAKS counterpart. A possible reason is that the CPCM-UAHF model is parametrized to a dated set of solvation data (derived from a proton free energy of solvation −1093.7 kJ mol^{-1} and estimated values for gas phase basicity).[33] Pliego has earlier highlighted this issue[4h] and recommended reparametrizing the (C)PCM-UAHF model using more reliable and updated solvation data. This might also explain why the MAEs (Table 2) of this solvation model are significantly higher (ca. 2 pH units) than the other solvation models. As such, the use of this model for the calculation of pK_as is discouraged. To summarize, our analysis indicates that the good agreement between direct and TC approaches for the SMD-M062X and CPCM-UAKS models reflects the similarity of the solvation contribution $\Delta\Delta G_S^*$ calculated at the DFT and G3(MP2)-RAD(+) levels of theory. In the SMD-HF model, the pK_as from the direct approach deviate significantly from the TC method as HF tends to result in a solute wave function that is overpolarized.

Aqueous pK_as of Amino Acids. On the basis of the above results, we have further calculated the first and second pK_as for a data set of eight amino acids (see the cycles in Figure 2) using the SMD-M062X, SMD-HF, and CPCM-UAKS models. These systems differ from the above test set in that they undergo structural rearrangements (tautomerization) upon solvation, and it is of interest to compare the performance of the TC and direct approach for these molecules. In our earlier study,[12] we

DOI: 10.1021/acs.jpcb.6b00164
J. Phys. Chem. B 2016, 120, 1319−1329

Table 4. Fixed Concentration SMD and Experimental (Where Available) Free Energies of Solvation (in kJ mol^{-1}) of Selected Systems Calculated at the HF, M06-2X, and G3(MP2)-RAD(+) Levels of Theory

		SMD-HF[a]		SMD-M062X[b]	
system	expt[d]	L = HF	H = G(+)[e]	L = M06-2X	H = G(+)[e]
CH_3OH	−21.4	−24.6	−17.8	−24.0	−18.3
CH_3O^-	−398.3	−356.4	−335.4	−342.4	−333.8
$\Delta\Delta G_S^*$[c]	−376.9	−331.8	−317.6	−318.4	−315.5
$C(CH_3)_3OH$	−18.9	−24.4	−18.6	−23.0	−18.4
$C(CH_3)_3O^-$		−323.6	−299.8	−308.2	−298.6
$\Delta\Delta G_S^*$[b]		−299.2	−281.1	−285.1	−280.2
C_6H_5OH	−27.7	−32.0	−23.6	−29.4	−22.8
$C_6H_5O^-$	−298.3	−277.2	−258.4	−264.6	−257.9
$\Delta\Delta G_S^*$[c]	−270.6	−245.2	−234.9	−235.2	−235.1
p-Me-C_6H_4OH		−29.5	−22.0	−27.9	−21.4
p-Me-$C_6H_4O^-$		−277.9	−257.8	−264.1	−257.4
$\Delta\Delta G_S^*$[c]		−248.3	−235.8	−236.2	−235.9
CH_3COOH	−28.0	−37.5	−25.8	−31.3	−25.1
CH_3COO^-	−323.4	−320.9	−297.7	−305.7	−296.9
$\Delta\Delta G_S^*$[c]	−295.4	−283.4	−271.9	−274.4	−271.8
C_6H_5COOH	−32.9	−37.8	−24.8	−31.3	−24.0
$C_6H_5COO^-$	−297.9	−298.2	−272.7	−280.9	−271.4
$\Delta\Delta G_S^*$[c]	−265.0	−260.3	−247.9	−249.6	−247.3
p-CN-$C_6H_4O^\bullet$		−41.2	−16.8	−29.3	−22.9
p-CN-$C_6H_4O^-$		−234.8	−217.3	−221.9	−216.2
$\Delta\Delta G_S^*$[c]		−193.6	−200.5	−192.6	−193.3
p-NMe_2-$C_6H_4O^\bullet$		−59.0	−38.9	−56.9	−48.5
p-NMe_2-$C_6H_4O^-$		−280.6	−261.3	−266.7	−260.6
$\Delta\Delta G_S^*$[c]		−221.6	−222.4	−209.8	−212.1
$(CH_3)_2C(O^\bullet)OH$		−55.5	−26.9	−32.0	−26.9
$(CH_3)_2C(O^-)OH$		−324.7	−298.3	−311.5	−299.3
$\Delta\Delta G_S^*$[c]		−269.2	−271.4	−279.5	−272.4
alanine-protonated		−325.3	−311.5	−314.8	−308.8
alanine-zwitterion		−81.9	−56.9	−74.4	−56.2
alanine-neutral		−55.8	−42.9	−47.7	−40.2
$\Delta\Delta G_S^*$[c] (P to Z)		243.4	254.6	240.4	252.6
$\Delta\Delta G_S^*$[c] (P to N)		269.5	268.6	267.1	268.6

[a]Calculations were performed on HF/6-31+G(d) optimized geometries. [b]Calculations were performed on M06-2X/6-31+G(d) optimized geometries. [c]Excludes contribution from free energy of solvation of proton. [d]From ref 32. [e]Abbreviation for G3(MP2)-RAD(+).

found the direct method provided a significant improvement compared to the TC approach for the SMD-M062X model. As shown in Figure 4, a similar trend is observed for the other solvation models where the MAE associated with the direct approach is generally lower than that of the TC approach. This

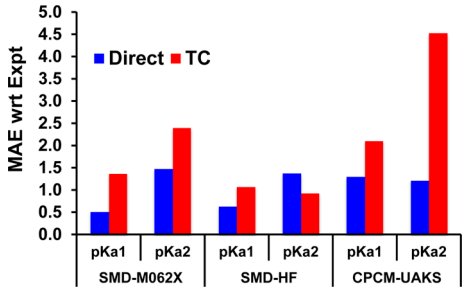

Figure 4. Mean absolute errors of the first and second pK_as of a test set of amino acids calculated using direct and TC approaches.

signifies that the solvation contribution to the reaction energy (eq 10) becomes more sensitive to the choice of level of theory when there are significant changes in geometry of the reactants (and/or products).

To better understand these results, we considered the SMD-M062X model and the first ionization of protonated alanine (P) as an example: the conjugate base can exist as a zwitterion (Z) or in its neutral (N) form, where the former is known to dominate in aqueous solution. The calculated free energies of solvation are shown in Table 4 (bottom five rows). For the P → Z reaction, the M06-2X and G(+) $\Delta\Delta G_S^*$ are 240 and 253 kJ mol^{-1}, respectively. For the P → N reaction, corresponding values are 267 and 269 kJ mol^{-1}, in much better agreement. As shown in Table 4, the SMD-M062X free energies of solvation show a very systematic deviation (ca. 6 kJ mol^{-1}) from the G(+) values for both protonated and neutral alanine. For the zwitterion, the deviation is significantly higher (ca. 18 kJ mol^{-1}) presumably because it also includes the tautomerization free energy that may be more sensitive to electron correlation and/or basis set effects. Thus, when the geometries of reactant and products are unaffected by solvation, there is better cancellation of errors in the solvation contribution computed at the low level of theory (L) that brings it into closer agreement with values computed at the high level (H). When this is not the case, a larger change in the solvation contribution (see eq 10) is expected as the electronic description of the solute is improved. We attribute the improvement afforded by the direct approach to the fact that the high-level calculations (i.e., electron correlation effects) are directly recovered on the chemically relevant solution phase species (zwitterions).

Cluster-Continuum Schemes. For a subset of 22 molecules, we further calculated their pK_as using the cluster-continuum scheme (cycle C in Figure 1) with up to three explicit water molecules for the SMD-M062X, SMD-HF, and CPCM-UAKS models. Table 5 summarizes the MAE with respect to experimental values. In all three models, increasing the degree of solvation (n = number of explicit water molecules) generally improves the mean accuracy of the directly calculated pK_as. The opposite trend is observed for the

Table 5. Mean Absolute Error of Cluster-Continuum pK_as Compared to Experiment

		SMD		SMD-HF		UAKS	
N[a]	$n$$H_2O$	direct	TC	direct	TC	direct	TC
22	0	5.9	5.7	5.7	4.6	6.3	6.9
22	1	5.1	5.9	5.3	5.2	5.8	8.6
19	2	4.9	7.3	4.7	5.7	5.8	11.7

[a]Number of molecules in data set.

DOI: 10.1021/acs.jpcb.6b00164
J. Phys. Chem. B 2016, 120, 1319−1329

TC approach. As a consequence, the deviation between direct and TC approaches increases with n. A possible explanation is that in the solution phase the water molecules in the first solvent shell can interact with the solvent (albeit implicitly in a polarizable continuum model), and the clustered ion is known to adopt a more open or "loose" structure.[4a] As noted above, solvation induced changes in reactant and/or product geometry can lead to larger deviations in direct and TC approaches.

Equation 11 shows the solvation contribution to the cluster-continuum scheme which is the major source of error in the TC calculations.

$$\Delta\Delta G_S^* = \Delta G_S^*(A(H_2O)_n) - \Delta G_S^*(HA) - n\Delta G_S^*(H_2O) \quad (11)$$

To better understand the trends in Table 5, we compared the calculated and experimental free energies of solvation of selected clustered ions. As explained before, continuum solvation models tend to underestimate the free energies of solvation of anions (Table 4) presumably because specific solute−solvent interactions are not modeled explicitly. Using methoxide as an example, increasing degree of solvation ($MeO^-\cdot(H_2O)_n$, n = 1−3) improves the accuracy associated with SMD-M062X and SMD-HF free energies of solvation, while the error rises monotonically for the CPCM-UAKS model (red line in Figure 5). On the other hand, the computed

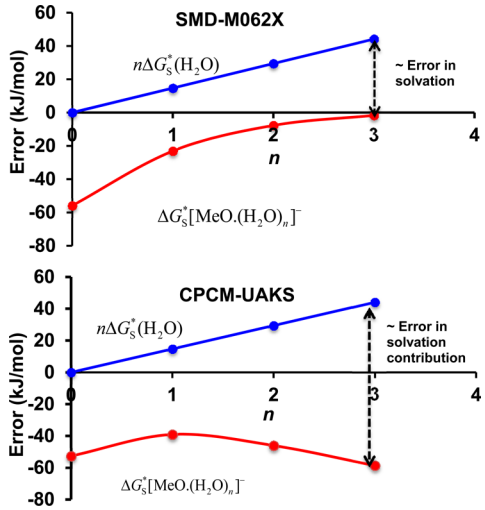

Figure 5. Signed errors (kJ mol^{-1}) in the calculated free energy of solvation of water and methoxide−water clusters. The error in the solvation contribution is approximately equal to the gap between the blue and red curves.

free energy of solvation of water (experiment −26.4 kJ mol^{-1})[34] is *overestimated* by all three solvation models SMD-M062X (−41.2 kJ mol^{-1}), SMD-HF (−41.0 kJ mol^{-1}), and CPCM-UAKS (−34.8 kJ mol^{-1}). As the number of reactant water molecules increases, the error in the calculated free energy of solvation of water contributes in a cumulative fashion to the solvation contribution. Since the free energies of solvation are under- and overestimated for the product (clustered ion) and reactant (water), respectively, these errors are compounded in the solvation contribution as shown in eq 11. This information is presented graphically for the methoxide anion in Figure 5. The error in the solvation contribution eq 11 can be estimated from the gap between the blue and red curves.

In the SMD-M062X model, the cumulative errors associated with the solvation free energy of water are mostly canceled by the improvement in the clustered ion. By comparison, the CPCM-UAKS model increasingly underestimates the free energy of solvation of the clustered ion with increasing degree of solvation. This explains the steep rise in MAE for the TC-UAKS approach (6.9−11.7 pH units with the addition of two water molecules). In the direct approach, the free energy change does not rely on the accuracy of the free energies of solvation, and its accuracy is retained (if not improved slightly) with the addition of explicit solvent molecules. Collectively, these results suggest that the direct approach when combined with a DFT-based solvation model provide a reliable and general alternative to the TC approach for the calculation of pK_as and reduction potentials of organic systems.

Enolization and Atom Transfer Reactions. In addition to pK_as and reduction potentials, we have also compared the performance of both approaches for neutral reactions such as the free energies of enolization and hydrogen or chlorine atom transfer. Figure 6 compares the mean and maximum absolute

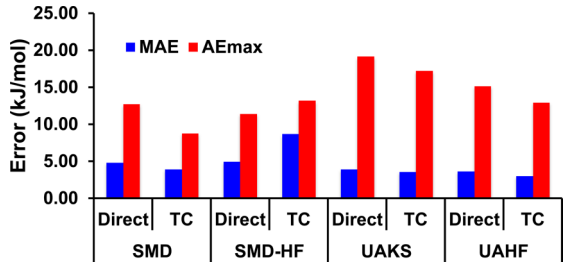

Figure 6. Comparison of mean and maximum absolute errors (in kJ mol^{-1}) of calculated tautomerization energies in water.

errors of 32 calculated keto−enol tautomerization free energies in water. This set of reactions was chosen from a data set compiled by Guthrie and Povar.[18] The compounds span a wide range in enol content, from cyclohexadienone where the enol is overwhelmingly favored to carboxylic acids, to esters where the enol is strongly disfavored.

For this set of reactions, we find again that the accuracies for direct and TC approaches are very comparable. Notably, the MAE is also significantly smaller for this class of reactions, ca. 5 kJ mol^{-1} across all solvation models. This is because the tautomerization reaction involves only neutral species, which continuum solvation models can predict their hydration free energies with reasonably high accuracy (within 4 kJ mol^{-1} of experiment for typical solutes).[24−26] These results are also very comparable to an earlier study that employed a parametrized IPCM solvation model.[18] Thus, the present results also demonstrate the utility of continuum solvation models to yield reasonably accurate reaction free energies for neutral organic compounds in aqueous solution.

We have further computed the free energies of hydrogen and chlorine atom transfer from chloroform to a series of six alkyl carbon centered radicals. In these reactions, the two processes proceeded in a competitive fashion and were found to occur under kinetic control.[19,35] As such, there is no thermodynamic data to compare with the theoretical calculations. Nonetheless, we observed for the set of 12 transfer energies, the values calculated from both approaches differed by less than 4 kJ mol^{-1} in all cases (Table S9 in Supporting Information). Collectively, the direct approach (when applied with a validated

DOI: 10.1021/acs.jpcb.6b00164
J. Phys. Chem. B 2016, 120, 1319−1329

DFT-based solvation model) offers a reliable and general alternative to calculating reaction energies in the solution phase for a broad range of systems.

Kinetics. *Reaction Barriers.* In addition to solution phase thermodynamics, it is also of interest to compare the performance of TC and direct approaches for the calculation of free energy barriers in the solution phase. We have compiled a test set of 83 transition states for various neutral, ionic and radical reactions from previous studies (see references in Table 1). As shown in Scheme 1, the set of ionic reactions include bimolecular nucleophilic substitution (SN2) and elimination (E2) as well as Michael addition reactions, while the radical reactions cover carbon-centered radical addition, radical cyclization, and hydrogen and chlorine atom transfer. Since most of these reactions were carried out in organic solvents, we will focus on the SMD-M062X solvation model in this section because the CPCM-UAKS/UAHF models have been optimized for aqueous solvent only.

Figure 7 compares the Gibbs free energies of activation between TC and direct approaches for the full set of reactions.

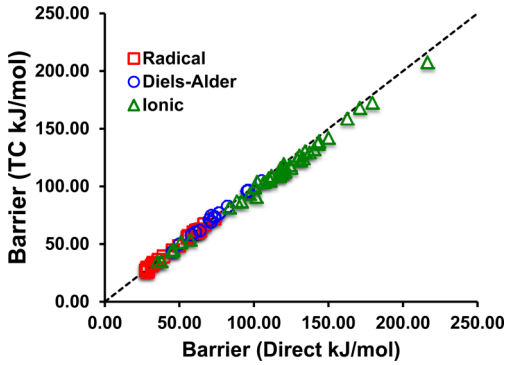

Figure 7. Correlation between Gibbs free energy barriers calculated using the direct and TC approach in conjunction with the SMD-M062X solvation model.

The results are very similar to those shown in Figure 3 where there is generally very good agreement between the two approaches. In the case of neutral Diels–Alder and radical addition and abstraction reactions, the MAD is about 1 kJ mol^{-1}. For comparison, ionic bimolecular SN2 and E2 reactions display larger MAD of about 4 kJ mol^{-1} with deviations as large as 10 kJ mol^{-1}. To better understand these results, we compared the effect of solvation on the geometries of these ionic transition states. We computed the RMSD between transition state geometries optimized in the gas and solution phase and observed a direct correlation with the magnitude of the deviation between TC and direct approach values (Table 6).

Notably, the large RMSD values are a consequence of the formation of a "loose" transition state geometry upon solvation where there is significant lengthening of the carbon center–nucleophile distance (ca. 0.25 Å). This increase in bond length is consistent with continuum solvation models' ability to stabilize separated charges, as the partial charges on the reacting carbon center and chlorine atoms increase with increasing bond distance.[37] As mentioned before, larger deviations between direct and TC approaches are expected when there are significant changes in geometry upon inclusion of bulk solvation effects. Table 6 shows the data for selected systems with available experimental data. The comparison indicates that where the deviation between TC and direct approaches is large (>5 kJ mol^{-1}), the latter generally yields free energy changes that are in better accord with experiment (iPr-Cl and tBu-Cl). These results are consistent with the pK_a calculations for amino acids.

SUMMARY AND CONCLUSIONS

We have carried out an extensive study comparing the performance of thermodynamic cycle (TC) and direct approaches for calculating free energy changes in the solution phase. This includes solution phase pK_as and standard reduction potentials, keto–enol tautomerization, and H/Cl atom transfer reactions. Additionally, free energy barriers of a range of neutral, ionic, and radical reactions were also computed. Several commonly used continuum solvation models (SMD-M062X, SMD-HF, CPCM-UAKS, CPCM-UAHF) were examined, and the results indicate that the direct approach when applied in conjunction with a DFT-based solvation model tends to give the best agreement with corresponding thermodynamic cycle calculations for a broad range of reactions. This is because the solvation contribution to the reaction energies computed at the DFT level is generally very similar to values calculated at a high level of theory such as G3(MP2)-RAD(+) composite procedure.

Table 6. Comparison of Calculated Gibbs Free Energy of Activation (kJ mol^{-1}) and Experiment for Selected SN2 Reactions

	ΔG^{act}(direct)	ΔG^{act}(TC)	AD	RMSD[d] (Å)	expt
CN(−)+EtCl[a]	117.7	116.1	1.6	0.04	92.3[e]
CN(−)+EtBr[a]	117.7	116.1	1.6	0.06	81.3[e]
CN(−)+EtI[a]	101.9	104.5	2.6	0.06	77.0[e]
CN(−)+EtTosyl[a]	119.8	119.7	0.1	0.06	86.2[e]
Cl(−)+MeCl[b]	100.1 (0.0)[c]	99.3 (0.0)[c]	0.7	0.01	0.0[f]
Cl(−)+EtCl[b]	111.5 (11.4)[c]	109.4 (10.1)[c]	2.1	0.03	9.3[f]
Cl(−)+iPrCl[b]	117.7 (17.6)[c]	112.4 (13.1)[c]	5.2	0.07	17.6[f]
Cl(−)+PrCl[b]	109.8 (9.7)[c]	107.4 (8.1)[c]	2.3	0.04	10.5[f]
Cl(−)+iBuCl[b]	117.3 (17.2)[c]	114.2 (14.9)[c]	3.0	0.03	14.9[f]
Cl(−)+tBuCl[b]	120.6 (20.5)[c]	113.5 (14.2)[c]	7.1	0.22	24.3[f]
Cl(−)+neopentylCl[b]	143.4 (43.3)[c]	139.2 (39.9)[c]	4.2	0.04	36.7[f]
Cl(−)+allylCl[b]	97.0 (−3.1)[c]	93.6 (−5.7)[c]	3.5	0.05	−0.7[f]
Cl(−)+benzylCl[b]	91.6 (−8.5)[c]	87.1 (−12.2)[c]	4.5	0.04	−3.4[f]

[a]In DMSO solution. [b]In acetonitrile solution. [c]Relative values in parentheses. [d]RMSD calculations exclude hydrogen atoms. [e]From ref 20a. [f]Relative to MeCl. From ref 36.

DOI: 10.1021/acs.jpcb.6b00164
J. Phys. Chem. B 2016, 120, 1319–1329

An interesting question arises when the TC and direct approaches deviate significantly, that is which approach is in better agreement with experiment? For HF-based solvation models, the TC approach performed better for pK_a calculations of alcohols and carboxylic acids mainly because the resulting free energies of solvation were in better agreement with experiment. For DFT-based solvation models, the direct approach tends to be in better agreement with experiment for the pK_as of amino acids and reaction barriers for certain SN2 and E2 reactions where solvation induced changes in geometry are significant. Presumably, this is because electron correlation and basis set effects are recovered on the solution phase species in their optimized geometries. It would be desirable to test this hypothesis more broadly; however, such systems are also relatively scarce, suggesting that direct calculation of free energy changes in a continuum solvation model offers a reliable alternative to the thermodynamic cycle approach for a broad range of "everyday" organic systems.

■ ASSOCIATED CONTENT

Supporting Information

The Supporting Information is available free of charge on the ACS Publications website at DOI: 10.1021/acs.jpcb.6b00164.

Tables of calculated and experimental pK_as, reduction potentials, enolization free energies and reaction barriers; a worked example showing how pK_as are computed through the TC and direct approaches (PDF)

■ AUTHOR INFORMATION

Corresponding Author

*E-mail: hojm@ihpc.a-star.edu.sg (J.H.).

Notes

The authors declare no competing financial interest.

■ ACKNOWLEDGMENTS

J.H. acknowledges support from the Agency for Science and Technology, the A*STAR Computational Resource Centre (ACRC) and Yale High Performance Computing facility for generous allocation of computing time. The work at BNL (M.Z.E.) was carried out under Contract DE-SC00112704 with the U.S. Department of Energy, Office of Science, Office of Basic Energy Sciences.

■ REFERENCES

(1) Skyner, R. E.; McDonagh, J. L.; Groom, C. R.; van Mourik, T.; Mitchell, J. B. O. A Review of Methods for the Calculation of Solution Free Energies and the Modelling of Systems in Solution. *Phys. Chem. Chem. Phys.* **2015**, *17*, 6174−6191.

(2) (a) Tomasi, J.; Mennucci, B.; Cammi, R. Quantum Mechanical Continuum Solvation Models. *Chem. Rev.* **2005**, *105*, 2999−3093. (b) Cramer, C. J.; Truhlar, D. G. Implicit Solvation Models: Equilibria, Structure, Spectra, and Dynamics. *Chem. Rev.* **1999**, *99* (8), 2161−2200. (c) Bashford, D.; Case, D. A. Generalized Born Models of Macromolecular Solvation Effects. *Annu. Rev. Phys. Chem.* **2000**, *51*, 129−152. (d) Orozco, M.; Luque, F. J. Theoretical Methods for the Description of the Solvent Effect in Biomolecular Systems. *Chem. Rev.* **2000**, *100*, 4187−4225.

(3) (a) Lin, C. Y.; Izgorodina, E. I.; Coote, M. L. First Principles Prediction of the Propagation Rate Coefficients of Acrylic and Vinyl Esters: Are We There Yet? *Macromolecules* **2010**, *43*, 553−560. (b) Truhlar, D. G.; Pliego, J. R., Jr. Transition State Theory and Chemical Reaction Dynamics in Solution. In *Conitnuum Solvation Models in Chemical Physics: From Theory to Applications*; Mennucci, B., Cammi, R., Eds.; Wiley: Chichester, 2008; pp 338−365. (c) Harvey, J. N. Ab initio Transition State Theory for Polar Reactions in Solution. *Faraday Discuss.* **2010**, *145*, 487−505. (d) Noble, B. B.; Coote, M. L. First Principles Modelling of Free-Radical Polymerization Kinetics. *Int. Rev. Phys. Chem.* **2013**, *32*, 467−513.

(4) (a) Ho, J.; Coote, M. L. A Universal Approach to Continuum Solvent pKa Calculations - Are We There Yet? *Theor. Chem. Acc.* **2010**, *125*, 3−21. (b) Ho, J.; Coote, M. L. First Principles Prediction of Acidities in the Gas and Solution Phase. *Comput. Mol. Sci.* **2011**, *1*, 649. (c) Shields, G. C.; Seybold, P. G. *Computational Approaches for the Prediction of pKa Values*; CRC Press: 2013. (d) Alongi, K. S.; Shields, G. C. Theoretical Calculations of Acid Dissociation Constants: A Review Article. *Annu. Rep. Comput. Chem.* **2010**, *6*, 113−138. (e) Keith, J. A.; Carter, E. A. Electrochemical Reactivities of Pyridinium in Solution: Consequences for CO_2 Reduction Mechanisms. *Chem. Sci.* **2013**, *4*, 1490−1496. (f) Chipman, D. M. Computation of pKa from Dielectric Continuum Theory. *J. Phys. Chem. A* **2002**, *106* (32), 7413−7422. (g) Klicic, J. J.; Friesner, R. A.; Liu, S.-Y.; Guida, W. C. Accurate Prediction of Acidity Constants in Aqueous Solution via Density Functional Theory and Self-Consistent Reaction Field Methods. *J. Phys. Chem. A* **2002**, *106* (7), 1327−1335. (h) Pliego, J. R. Thermodynamic Cycles and the Calculation of pKa. *Chem. Phys. Lett.* **2003**, *367*, 145−149. (i) Kelly, C. P.; Cramer, C. J.; Truhlar, D. G. Adding Explicit Solvent Molecules to Continuum Solvent Calculations for the Calculation of Aqueous Acid Dissociation Constants. *J. Phys. Chem. A* **2006**, *110* (7), 2493−2499. (j) Marenich, A. V.; Ding, W.; Cramer, C. J.; Truhlar, D. G. Resolution of a Challenge for Solvation Modeling: Calculation of Dicarboxylic Acid Dissociation Constants Using Mixed Discrete−Continuum Solvation Models. *J. Phys. Chem. Lett.* **2012**, *3*, 1437−1442.

(5) (a) Marenich, A. V.; Ho, J.; Coote, M. L.; Cramer, C. J.; Truhlar, D. G. Computational Electrochemistry: Prediction of Liquid-Phase Reduction Potentials. *Phys. Chem. Chem. Phys.* **2014**, *16*, 15068−15106. (b) Rulíšek, L. On the Accuracy of Calculated Reduction Potentials of Selected Group 8 (Fe, Ru, and Os) Octahedral Complexes. *J. Phys. Chem. C* **2013**, *117*, 16871−16877. (c) Guerard, J. J.; Arey, J. S. Critical Evaluation of Implicit Solvent Models for Predicting Aqueous Oxidation Potentials of Neutral Organic Compounds. *J. Chem. Theory Comput.* **2013**, *9*, 5046−5058. (d) Schmidt am Busch, M.; Knapp, E.-W. One-Electron Reduction Potential for Oxygen- and Sulfur-Centered Organic Radicals in Protic and Aprotic Solvents. *J. Am. Chem. Soc.* **2005**, *127*, 15730−15737. (e) Baik, M. H.; Friesner, R. A. Computing Redox Potentials in Solution: Density Functional Theory as a Tool for Rational Design of Redox Agents. *J. Phys. Chem. A* **2002**, *106*, 7407−7412. (f) Psciuk, B. T.; Schlegel, B. H. Computational Prediction of One-Electron Reduction Potentials and Acid Dissociation Constants for Guanine Oxidation Intermediates and Products. *J. Phys. Chem. B* **2013**, *117*, 9518−9531. (g) Psciuk, B. T.; Lord, R. L.; Munk, B. H.; Schlegel, B. H. Theoretical Determination of One-Electron Oxidation Potentials for Nucleic Acid Bases. *J. Chem. Theory Comput.* **2012**, *8*, 5107−5123.

(6) (a) Jensen, J. H. Predicting Accurate Absolute Binding Energies in Aqueous Solution: Thermodynamic Considerations for Electronic Structure Methods. *Phys. Chem. Chem. Phys.* **2015**, *17*, 12441−12451. (b) Grimme, S. Supramolecular Binding Thermodynamics by Dispersion-Corrected Density Functional Theory. *Chem. - Eur. J.* **2012**, *18*, 9955−9964.

(7) Ho, J. Predicting pKa in Implicit Solvents: Current Status and Future Directions. *Aust. J. Chem.* **2014**, *67*, 1441−1460.

(8) Ho, J.; Klamt, A.; Coote, M. L. Comment on the Correct Use of Continuum Solvent Models. *J. Phys. Chem. A* **2010**, *114*, 13442−13444.

(9) Ribeiro, R. F.; Marenich, A. V.; Cramer, C. J.; Truhlar, D. G. Use of Solution-Phase Vibrational Frequencies in Continuum Models for the Free Energy of Solvation. *J. Phys. Chem. B* **2011**, *115*, 14556−14562.

(10) Curtiss, L. A.; Redfern, P. C.; Raghavachari, K.; Rassolov, V.; Pople, J. A. Gaussian-3 Theory using Reduced Møller-Plesset Order. *J. Chem. Phys.* **1999**, *110*, 4703−4709.

(11) Montgomery, J. A., Jr.; Frisch, M. J.; Ochterski, J. W.; Petersson, G. A. A Complete Basis Set Model Chemistry. VI. Use of Density Functional Geometries and Frequencies. *J. Chem. Phys.* **1999**, *110* (6), 2822−2827.
(12) Ho, J. Are Thermodynamic Cycles Necessary for Continuum Solvent Calculation of pKas and Redox Potentials? *Phys. Chem. Chem. Phys.* **2015**, *17*, 2859−2868.
(13) (a) Casasnovas, R.; Ortega-Castro, J.; Frau, J.; Donoso, J.; Munoz, F. Theoretical pKa Calculations with Continuum Model Solvents, Alternative Protocols to Thermodynamic Cycles. *Int. J. Quantum Chem.* **2014**, *114*, 1350−1363. (b) Sastre, S.; Casanovas, R.; Munoz, F.; Frau, J. *Theor. Chem. Acc.* **2013**, *132*, 1310.
(14) Henry, D. J.; Sullivan, M. B.; Radom, L. G3-RAD and G3X-RAD: Modified Gaussian-3 (G3) and Gaussian-3X (G3X) Procedures for Radical Thermochemistry. *J. Chem. Phys.* **2003**, *118*, 4849−4860.
(15) Gupta, M.; da Silva, E. F.; Svendsen, H. F. Explicit Solvation Shell Model and Continuum Solvation Models for Solvation Energy and pKa Determination of Amino Acids. *J. Chem. Theory Comput.* **2013**, *9*, 5021−5037.
(16) Bryantsev, V. S.; Diallo, M. S.; Goddard, W. A., III Calculation of Solvation Free Energies of Charged Solutes Using Mixed Cluster/Continuum Models. *J. Phys. Chem. B* **2008**, *112*, 9709−9719.
(17) Ho, J.; Coote, M. L. pKa Calculation of Some Biologically Important Carbon Acids: An Assessment of Contemporary Theoretical Procedures. *J. Chem. Theory Comput.* **2009**, *5*, 295−306.
(18) Guthrie, J. P.; Povar, I. Equilibrium Constants for Enolization in Solution by Computation Alone. *J. Phys. Org. Chem.* **2013**, *26*, 1077−1083.
(19) Ho, J.; Zheng, J.; Meana-Paneda, R.; Truhlar, D. G.; Ko, E. J.; Savage, G. P.; Williams, C. M.; Coote, M. L.; Tsanaksidis, J. Chloroform as a Hydrogen Atom Donor in Barton Reductive Decarboxylation Reactions. *J. Org. Chem.* **2013**, *78*, 6677−6687.
(20) (a) Westaway, K. C.; Fang, Y.-r.; MacMillar, S.; Matsson, O.; Poirier, R. A.; Islam, S. M. Determining the Transition-State Structure for Different SN2 Reactions Using Experimental Nucleophile Carbon and Secondary Alpha-Deuterium Kinetic Isotope Effects and Theory. *J. Phys. Chem. A* **2008**, *112*, 10264−10273. (b) Krenske, E. H.; Petter, R. C.; Zhu, Z.; Houk, K. N. Transition States and Energetics of Nucleophilic Additions of Thiols to Substituted α,β-unsaturated Ketones: Substituent Effects Involve Enone Stabilization, Product Branching, and Solvation. *J. Org. Chem.* **2011**, *76*, 5074−5081. (c) Rablen, P. R.; McLarney, B. D.; Karlow, B. J.; Schneider, J. E. How Alkyl Halide Structure Affects E2 and SN2 Reaction Barriers: E2 Reactions Are as Sensitive as SN2 Reactions. *J. Org. Chem.* **2014**, *79*, 867−879.
(21) Tang, S.-Y.; Shi, J.; Guo, Q.-X. Accurate Prediction of Rate Constants of Diels-Alder Reactions and Application to Design of Diels-Alder Ligation. *Org. Biomol. Chem.* **2012**, *10*, 2673−2682.
(22) Lobachevsky, S.; Schiesser, C. H.; Lin, C. Y.; Coote, M. L. First-Principles Prediction of Rate Coefficients for Free-Radical Cyclization Reactions at Selenium. *J. Phys. Chem. A* **2008**, *112*, 13622−13627.
(23) Frisch, M. J.; Trucks, G. W.; Schlegel, H. B.; Scuseria, G. E.; Robb, M. A.; Cheeseman, J. R.; Scalmani, G.; Barone, V.; Mennucci, B.; Petersson, G. A.; et al. *Gaussian 09, Revision D.01*; Gaussian, Inc.: Wallingford, CT, 2009.
(24) Marenich, A. V.; Cramer, C. J.; Truhlar, D. G. Universal Solvation Model Based on Solute Electron Density and a Continuum Model of the Solvent Defined by the Bulk Dielectric Constant and Atomic Surface Tensions. *J. Phys. Chem. B* **2009**, *113*, 6378−6396.
(25) Takano, Y.; Houk, K. N. Benchmarking the Conductor-Like Polarizable Continuum Model (CPCM) for Aqueous Solvation Free Energies of Neutral and Ionic Organic Molecules. *J. Chem. Theory Comput.* **2005**, *1* (1), 70−77.
(26) Barone, V.; Cossi, M.; Tomasi, J. A New Definition of Cavities for the Computation of Solvation Free Energies by the Polarizable Continuum Model. *J. Chem. Phys.* **1997**, *107* (8), 3210−3221.
(27) Zhao, Y.; Truhlar, D. G. The M06 suite of density functionals for main group thermochemistry, thermochemical kinetics, noncovalent interactions, excited states, and transition elements: two new functionals and systematic testing of four M06-class functionals and 12 other functionals. *Theor. Chem. Acc.* **2008**, *120* (1−3), 215−241.
(28) Becke, A. D. Density-Functional Thermochemistry. III. The Role of Exact Exchange. *J. Chem. Phys.* **1993**, *98* (7), 5648−5652.
(29) Hehre, W. J.; Radom, L.; Schleyer, P. v. R.; Pople, J. A. *Ab Initio Molecular Orbital Theory*; Wiley: New York, 1986.
(30) Cammi, R. Coupled-Cluster Theory for the Polarizable Continuum Model. III. A Response Theory for Molecules in Solution. *Int. J. Quantum Chem.* **2012**, *112*, 2547.
(31) Ponder, J. W.; Case, D. A. Force Fields for Protein Simulations. *Adv. Protein Chem.* **2003**, *66*, 27−85.
(32) Pliego, J. R., Jr.; Riveros, J. M. Gibbs Energy of Solvation of Organic Ions in Aqueous and Dimethyl Sulfoxide Solutions. *Phys. Chem. Chem. Phys.* **2002**, *4* (9), 1622−1627.
(33) Pearson, R. G. Ionization Potentials and Electron Affinities in Aqueous Solution. *J. Am. Chem. Soc.* **1986**, *108*, 6109−6114.
(34) Camaioni, D. M.; Schwerdtfeger, C. A. Comment on "Accurate Experimental Values for the Free Energies of Hydration of H+, OH-, and H3O+. *J. Phys. Chem. A* **2005**, *109*, 10795.
(35) Ko, E. J.; Savage, G. P.; Williams, C. M.; Tsanaktsidis, J. Reducing the Cost, Smell, and Toxicity of the Barton Reductive Decarboxylation: Chloroform as the Hydrogen Atom Source. *Org. Lett.* **2011**, *13*, 1944−1947.
(36) (a) Streitwieser, A., Jr. Solvolytic Displacement Reactions At Saturated Carbon Atom. *Chem. Rev.* **1956**, *56*, 571−752. (b) Charton, M. Steric Effects. III. Bimolecular Nucleophilic Substitution. *J. Am. Chem. Soc.* **1975**, *97*, 3694−3697.
(37) (a) Kim, Y.; Cramer, C. J.; Truhlar, D. G. Steric Effects and Solvent Effects on SN2 Reactions. *J. Phys. Chem. A* **2009**, *113*, 9109−9114. (b) Chen, X.; Regan, C. K.; Craig, S. L.; Krenske, E. H.; Houk, K. N.; Jorgensen, W. L.; Brauman, J. I. Steric and Solvation Effects in Ionic S(N)2 Reactions. *J. Am. Chem. Soc.* **2009**, *131*, 16162−16170.

DOI: 10.1021/acs.jpcb.6b00164
J. Phys. Chem. B 2016, 120, 1319−1329